American Mineralogist, Volume 69, pages 104–111, 1984

Enumeration of 4-connected 3-dimensional nets and classification of framework silicates: linkages from the two $(5^2.8)_2(5.8^2)_1$ 2D nets

JOSEPH V. Smith

Department of the Geophysical Sciences
The University of Chicago, Chicago, Illinois 60637

AND J. MICHAEL BENNETT

Union Carbide Corporation
Tarrytown, New York 10591

Abstract

Two topologically distinct 3-connected 2D nets can be developed from pentagons and octagons, and the centered one can be distorted into an oblique net which is polytypic with the zigzag net. Many infinite series of polytypic 4-connected 3D nets were enumerated by addition of up–down linkages to the 3-connected nodes, and by conversion of horizontal branches of the two 2D nets into crankshaft and zigzag chains. Forty of the simpler nets were selected for detailed description, and four are represented by bikitaite, dachiardite, epistilbite and the $CsAlSi_5O_{12}$ structure. Some of the nets can also be described using other 2D nets as a basis: particularly interesting theoretically is a polytypic net containing pentagons and heptagons. All 3D nets obtained from the pentagon–octagon 2D nets by conversion of horizontal branches into saw chains are too complex and distorted to be described. Some of the polytypic series of nets are polytypic between series as well as within a series.

Introduction

Simple 2D nets were used as the basis of 4-connected 3D nets enumerated in the first four papers of this series (Smith, 1977, 1978, 1979; Smith and Bennett, 1981). The present paper provides a selected list of 3D frameworks derived from the centered and zigzag 2D nets with $(5^2.8)_2(5.8^2)_1$ nodes. In the first subgroup, a vertical branch is added to each 3-connected node and the choice of upward or downward corresponds to a two-color enumeration. Distortion of a 2D net occurs when a model is made from tetrahedral stars and plastic tubing; in particular, a horizontal branch between adjacent up and down branches turns into a crankshaft chain. Other 3D nets are obtained by conversion of a horizontal branch into a zigzag or a saw chain. Because all known natural and synthetic materials with framework structures are structurally elegant, complex inelegant nets with low symmetry and many types of nodes are deliberately omitted. The choice between selection and rejection is arbitrary, and a few complex structures are listed for safety. Cell dimensions were measured directly from models made of plastic tetrahedral stars linked 3.1 cm apart by Tygon tube segments; considerable variations can be expected in real crystal structures as the branches bend around nodes in response to physical and chemical forces.

Polytypic relation between the centered and zigzag nets

The obvious geometrical arrangement of the $(5^2.8)_2$ $(5.8^2)_1$ nodes produces a *centered* net with space group *cmm* (Fig. 1) in which octagon D lies at the center of a rectangular unit cell defined by ABA′B′. Each of the pentagons obeys a mirror line of symmetry. The ideal rectangular net can be homogeneously deformed into an oblique net (space group *p*2) in which A → G, B → H, D →H′, E → L, C → I, F → J. The unit cell becomes a parallelogram defined by GHG′H′, and the mirror lines are lost. Although K and L, and I and J, are in a mirror relation, the octagons are not. The zigzag net is topologically distinct from the centered/oblique nets; thus octagons N and O match G and H, but pentagons T and U replace M. The zigzag net has a rectangular unit cell outlined by NPN′P′ and the zigzag arrangement of octagons and pentagons gives the space group *pgm*. Polytypism can occur between the oblique and zigzag nets because they can be attached along lines of type dd to give an infinite number of combinations. The 3D nets will be arranged in the figures to show this polytypic relation;

0003–004X/84/0102–0104$02.00

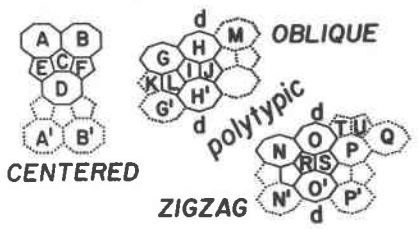

Fig. 1. Topological and geometrical relations between the centered/oblique and zigzag nets based on octagons and pentagons.

however, Table 1 gives cell dimensions only for the centered arrangement and not for the oblique one.

Addition of up-down linkages

Figure 2 shows plans of the simpler 3D nets formed by addition of up-down linkages to the 2D nets. Fourteen 3D nets (Table 1; 103, 220–232) were selected from the infinite number of two-color combinations from the centered net, and nine were selected for the two-color combinations of the zigzag net (Table 1; 223–241). Seven pairs (220/233; 103/234; 222/235; 223/236; 227/237; 229/238; 231/239) are related polytypically via the oblique (o) distortion of the centered (c) net, as shown by the adjacent triplets in Figure 2.

It must be emphasized that these 23 nets were chosen empirically out of an infinite number of possible combinations. To illustrate the complexity, Table 2 provides a systematic enumeration of 3D nets obtained from the centered 2D net with the restriction that the color (*i.e.*, up or down) is constant in the horizontal direction. There are eight rows to consider (1–8, extreme upper left, Fig. 2). If all have the same color with a run sequence of 8, a double-sheet structure (Table 2, first line) is obtained in which a 2D net with UUUUUUUU linkages is cross-

Table 1. Properties of nets

Arbitrary number	Z_t		Z_c	Highest space group	a	b	c	γ
					Angstrom			
220	12	$(4^35^26)_2(4^258^210)$	24	Imam	9	19	7.5	
103*	12	$(4^25^267)_2(4^258^3)_1$	24	Amnm	9	19	7.5	
221	12	$(45^26^28)_2(56^5)_1$	24	Amnm	9	19	7.5	
222	12	$(4^25^268)_2(53^38^2)_1$	24	Imam	9	19	7.5	
223	12	$(4^25^268)_2(458^4)_1$	24	Cmmm	9	19	7.5	
224	12	$(4^25^26^2)_2(4^2568^2)_1$ $(45^2678)_2(56^48)_1$	24	Im2m	9	19	7.5	
225	12	$(4^25^268)_2(56^38^2)_1$	24	Imam	9	19	7.5	
226	12	$(45^26^28)_2(456^28^2)_1$	24	Immm	9	19	7.5	
227	12	$(45^268)_1(4^256^28)_1(45^2678)_1$	12	P112/m	7.5	10	9	110°
228	12	$(4^25^268)_1(4^256^28)_1(45^267^2)_1$	24	Immb	9	19	7.5	
229	12	$(45^26^3)_1(5^26^4)_1$	24	A112/m	10	15	9	120°
230	24	$(45^26^3)_1(5^26^4)_1(56^5)_1$	48	Bbcm	16	19	9	
231	12	$(4^25^267)_1(4^25^28^2)_1(4^2568^2)_1$	24	A112/m	10	15	9	112°
232	24	$(4^25^267)_2(4^2568^2)_1$	48	Bbmm	15	19	9	
233	24	$(4^35^26)_2(4^258^210)_1$	48	Amam	14	20	9	
234	24	$(4^25^267)_2(4^258^3)_1$	24	Pnmm	10	14	9	
235	24	$(4^356^2)_1(4^25^267)_2$	48	Amam	14	20	9	
236	24	$(4^35^26)_1(4^25^268)_2$ $(45^26^3)_1(4568^3)_2$	24	Pbmm	10	14	9	
237	24	$(4^25^268)_1(4^256^28)_1(45^267^2)_1$	24	Pbmm	10	14	9	
238	24	$(45^26^3)_1(5^26^4)_1(56^5)_1$	24	Pnmm	10	14	9	
239	24	$(4^25^267)_1(4^25^278)_1(4^25678)_1$	24	Pbmm	10	14	9	
240	24	$(45^26^3)_1(456^28^2)_1(5^26^4)_1$	24	Pbmm	10	14	9	
241	24	$(45^26^3)_1(5^26^4)_1(56^5)_1$	48	Amam	14	20	9	
98	6	$(5^468^2)_2(56^5)_1$	12	Cmcm	7.5	15	5	

linked to a 2D net with DDDDDDDD linkages. When the first four rows of branches point up and the next four rows point down (UUUUDDDD), net 220 (Fig. 2, top left) is obtained; its sequences around the 8- and 5-rings are UUDDDDUU and UUUUU. The run sequence of 2U, 2D, 2U, 2D yields net 103 already given by Smith (1978), and run sequence UDUDUDUD gives net 221. Out of the combinations with run lengths of 4, 2 and 1 only the nets 222–226 are simple.

Nets 227–232 are shown because of special structural features. Net 227 has chains of edge-sharing 4-rings (unmarked nodes) crosslinked by parallel 4-rings (two dots) in a pattern with monoclinic symmetry. Its polytypic relative, net 228, has undulating chains of 4-rings crosslinked by a zigzag pattern of 4-rings. Nets 231 and 232 are composed entirely of chains of edge-sharing 4-rings at two levels. Finally nets 229 and 230 are interesting because U and D alternate around the 8-rings; alternation is not possible around a 5-ring, and a 4-ring is inserted between adjacent 5-rings.

Nine nets were chosen with up-down linkages from the 2D zigzag net. Nets 233–239 are related polytypically to centered nets 220, 103, 222–231 via an oblique distortion of each centered net. Net 241 is characterized by alternation of nodes around each 8-ring, and net 240 by a 4-ring bridge between each pair of adjacent 8-rings.

The following details appeared when models were built from tetrahedral stars and plastic tubes. After the 3D net has adjusted its shape (but not its connectivity), each pair of adjacent dissimilar nodes in Figure 2 represents a crankshaft chain (c) while adjacent similar nodes represent 4-rings arranged like stepping stones (s4s). Because

Table 1. (cont.)

Arbitrary number	Z_t		Z_c	Highest space group	a	b	c	γ
					Angstrom			
242	12	$(5^4 68)_1(5^3 6^3)_1(5^2 6^3 8)_1$	24	Bbmm	14	16	5	
243	6	$(5^4 68)_1(5^3 6^3)_1(5^2 6^3 8)_1$	12	A112/m	8	14	5	108°
244	12	$(5^5 8)_1(5^4 68)_1(56^5)_1$	12	Pnmm	9	13	5	
245	12	$(5^4 68)_1(5^3 6^3)_1(5^2 6^3 8)_1$	12	Pbmm	9	13	5	
246	12	$(4^2 5^3 7)_4(5^4 8^2)_1(5^3 8^2 10)_1$	24	A112/m	10	18	7.5	107°
247	24	$(4^2 5^3 7)_4(5^4 8^2)_1(5^3 8^2 10)_1$	24	Pncm	10	17	7.5	
248	12	$(45^3 7^2)_1(5^5 7)_1(5^4 67)_1$	24	A112/m	10	18	7.5	107°
249	24	$(45^3 7^2)_1(5^5 7)_1(5^4 67)_1$	24	Pnmm	10	18	7.5	
250	12	$(45^3 7^2)_1(5^5 7)_1(5^4 67)_1$	24	B112/m	9	10	18	125°
	(also pseudo-orthorhombic cell a 14 b 18 c 10)							
251	24	$(45^3 7^2)_1(5^5 7)_1(5^4 67)_1$	96	Fddd	15	36	10	
252	24	$(5^5 7)_1(5^4 67)_1(5^3 7^3)_1$	24	Pnam	10	18	7.5	
253	12	$(5^5 7)_1(5^4 67)_1(5^3 7^3)_1$	24	A112/m	10	18	7.5	110°
	(also pseudo-orthorhombic cell a 10 b 36 c 7.5)							
254	12	$(5^5 7)_1(5^4 67)_1(5^3 7^3)_1$	24	A112/a	9	10	18	120°
	(also pseudo-orthorhombic cell a 10 b 15 c 18)							
255	24	$(5^4 7)_1(5^4 67)_1(5^3 7^3)_1$	96	Fddd	15	36	10	
256	12	$(45^3 7^2)_4(5^4 7^2)_1(5^3 7^3)_1$	24	Pnnm	10	18	7.5	
257	12	$(45^3 7^2)_1(5^4 7^2)_1(5^3 7^3)_1$	24	A112/m	10	18	7.5	106°

*Originally described with monoclinic half-cell.

Type	Name	Reference	Space Group	Cell Dimensions a	b	c	
98	bikitaite	Kocman et al. (1974)	$P112_1$	7.60	8.61	4.96	γ114°
242	$CsAlSi_5O_{12}$	Araki (1980)	Bbm2	13.83	16.78	5.02	
248	dachiardite	Gottardi and Meier (1963)	C12/m1	18.7	7.5	10.3	β108°
250	epistilbite	Perrotta (1967)	C12/m1	8.9	17.7	10.2	β124°

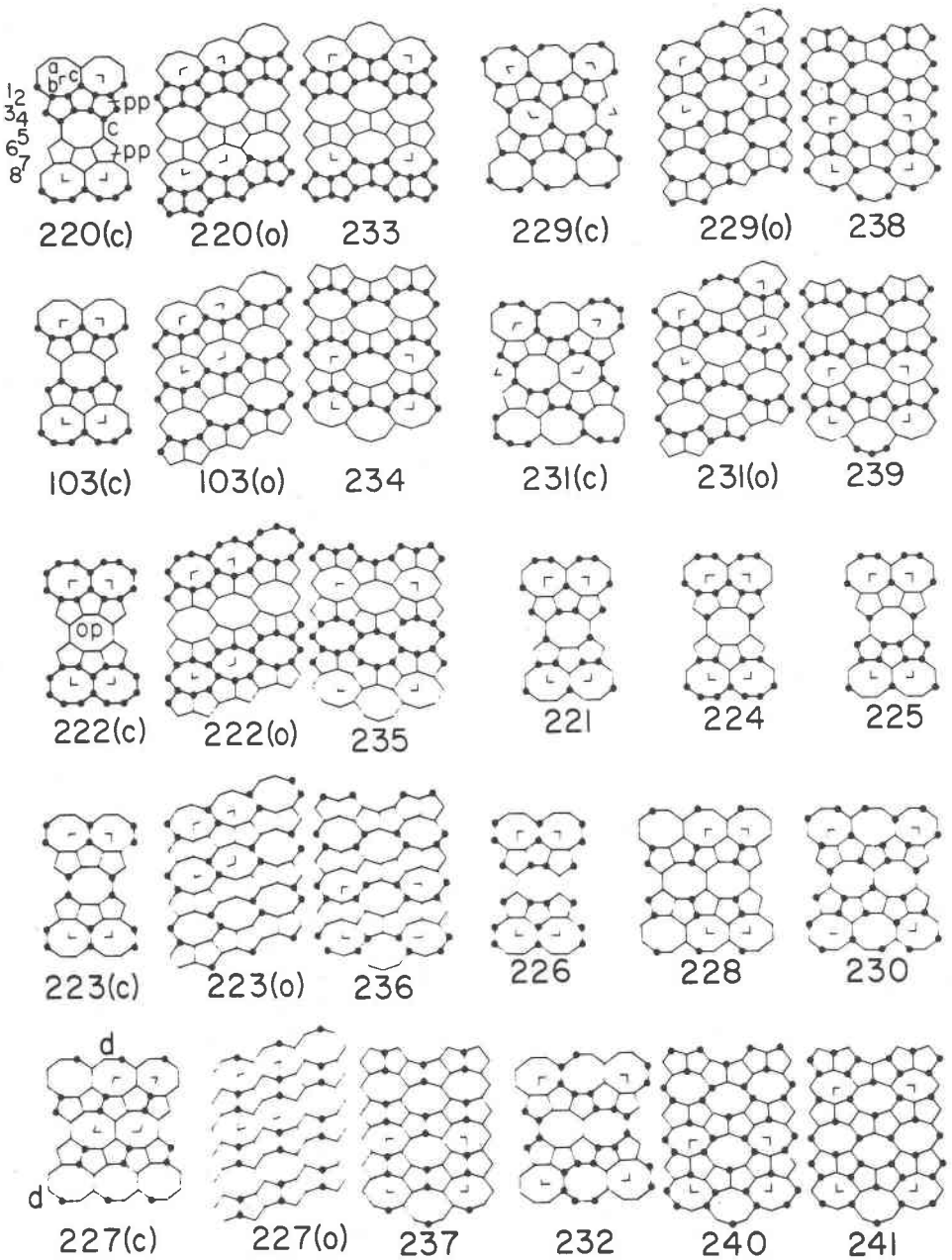

Fig. 2. Selected 3D nets obtained by addition of up–down linkages to the centered (c)/oblique (o) and zigzag nets. op octagonal prism, pp pentagonal prism.

6-rings in molecular sieves are permeable only by small molecules, emphasis will be placed on larger rings, especially in multiply-connected channel and cage systems. Net 220 consists of zigzag chains of face-sharing pentagonal prisms (pp) along the **c**-axis crosslinked by crankshaft chains along **a**. One-dimensional channels are bounded by elongated 12-rings. Net 221 contains crankshaft chains parallel to the *a*-axis (Fig. 2), and the **c**-axis projection (Fig. 3) shows saw(s) and c chains projecting onto a 6^3 net. The 1-dimensional channel system is limited by 8-rings. Net 222 contains chains of face-sharing octagonal prisms along the **c**-axis crosslinked by c chains along the **a**-axis. The 2D channel system is limited by elongated 12-rings perpendicular to **c** and 8-rings perpendicular to **a**. Net 233 projects down the **c**-axis onto a 4.8^2 net (Fig. 3), and its 3D channel system is limited by 8-rings. Nets 224–227 project down the **c**-axis onto complex 2D nets with 4-, 6-, and 8-rings, not shown in Figure 3, but the zigzag feature of the polytypic variant 228 of net 227 eliminates this property. Net 229 contains zigzag chains along the **c**-

Table 2. Enumeration of up-down 3D nets from $(5^2.8)_2$. $(5.8^2)_1$ net. Subgroup with constant color in 8.8 direction

Sequence	Pattern	Label	Sequence	Pattern	Label
8	UUUUUUUU	sheet	211211	UUDUDDUD	224
44	UUUUDDDD	220	211121	UUDUDUUD	unlisted
2222	UUDDUUDD	103	211112	UUDUDUDD	unlisted
11111111	UDUDUDUD	221	122111	UDDUUDUD	unlisted
422	UUUUDDUU	unlisted	121211	UDDUDDUD	unlisted
242	UUDDDDUU	222	121121	UDDUDUUD	225
41111	UUUUDUDU	unlisted	112211	UDUUDDUD	unlisted
14111	UDDDDUDU	unlisted	2111111	UUDUDUDU	unlisted
11411	UDUUUUDU	unlisted	1211111	UDDUDUDU	unlisted
22211	UUDDUUDU	unlisted	1121111	UDUUDUDU	unlisted
22121	UUDDUDDU	unlisted	1112111	UDUDDUDU	226
21221	UUDUUDDU	unlisted	4211	UUUUDDUD	unlisted
12221	UDDUUDDU	223	4121	UUUUDUUD	unlisted
22112	UUDDUDUU	unlisted	4112	UUUUDUDD	unlisted
21212	UUDUUDUU	unlisted	2411	UUDDDDUD	unlisted
221111	UUDDUDUD	unlisted	1421	UDDDDUUD	unlisted
212111	UUDUUDUD	unlisted	1412	UDDDDUDD	unlisted

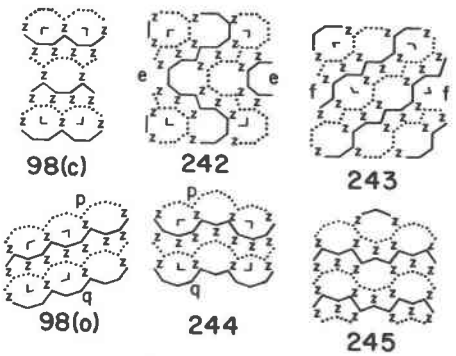

Fig. 4. Selected 3D nets obtained by addition of zigzag (z) linkages to the centered (c)/oblique (o) and zigzag 2D nets. Continuous and dotted lines show chains of horizontal linkages at two levels related by the vertical zigzag chains. Net 98(c) can be distorted to 98(o) which is polytypic along pq with zigzag net 244. Nets 242 and 243 are polytypic across ee and ff.

axis, and projects onto a 6^3 net (not shown in Fig. 3); its unconnected channels are walled by 6-rings and limited by 8-rings. The channels in net 230 are similar. Net 231 projects down its **b**-axis onto a 4.8^2 net, and its 3D channel system is limited by non-planar 8-rings. Net 232 has an even more complex 3D channel system also limited by non-planar 8-rings.

Net 233 contains horizontal zigzag chains of face-sharing pentagonal prisms at two levels crosslinked by vertical crankshaft chains to give elliptical channels spanned by 12-rings and interconnected by 8-rings. The zigzag chains of 4-rings in net 234 are crosslinked by vertical crankshaft chains to give a 2D corrugated channel system limited by 8-rings. Net 239 has a different type of 4-ring chain. Net 235 contains elliptical channels limited by 12-rings and interconnected via the face-sharing octagonal prisms.

Net 236 contains 4-rings (pairs of dots) as bridges between horizontal zigzag chains of 4-rings (unmarked nodes), and its 3D channel system is limited by 8-rings. Net 237 has a 4-ring bridge between each pair of 5-rings, while net 238 has 4-rings alternating with crankshafts. Net 238 also has alternation of U and D around each 8-ring, as also does net 241. Nets 238 and 240 have 4-ring bridges between adjacent 8-rings. All these nets have complex channel systems limited by 8-rings. Net 238 projects down its **a**-axis onto a 6^3 net.

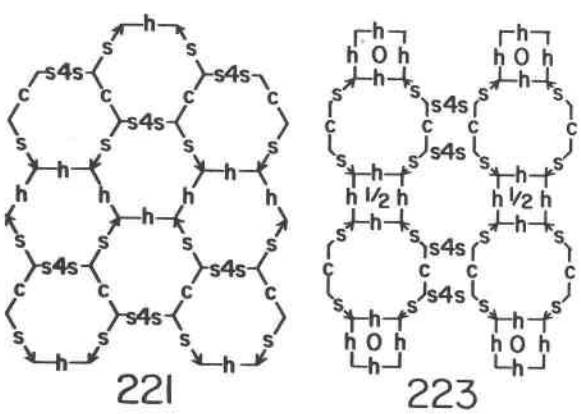

Fig. 3. Alternative projections of two nets from Fig. 2. Compare with Figs. 9 and 12 of Smith (1979). c crankshaft, h horizontal branch, s saw, s4s 4-rings in stepping-stone pattern.

Addition of zigzag chains

Figure 4 shows how vertical zigzag chains (z) can be combined with the centered/oblique and zigzag 2D nets. Because a horizontal branch of a 3-connected 2D net is converted into two inclined branches (zig and zag) of a zigzag chain, the two adjacent branches of the 2D net cannot be converted into zigzag branches; otherwise the 3D net would have more than 4 connections at each node. Each 4-connected node of the nets in Figure 4 lies at the intersection of one z chain and two horizontal branches. Continuous and dotted lines distinguish between the two levels of the horizontal branches. Net 98 (bikitaite) was already listed in Smith (1979) because it can also be described with a 6^3 2D net modified by crankshaft and saw chains. The centered/oblique 2D net yields two more 3D nets based on the choices for placement of three z chains in edge-shared pentagons. Net 242 is found in the structure of $CsAlSi_5O_{12}$ (Araki, 1980), and can be obtained from net 232 by replacement of each c chain (branch between dissimilar nodes; Fig. 2, middle bottom) by a z chain. Net 243 is similarly related to net 231; note that the chains are depicted in different diagonal directions. Nets 242 and 243 are polytypic across the boundaries ee and ff.

All these nets have isolated channels spanned by non-planar 8-rings. Net 243 nearly projects down its [110] axis onto a 6^3 net.

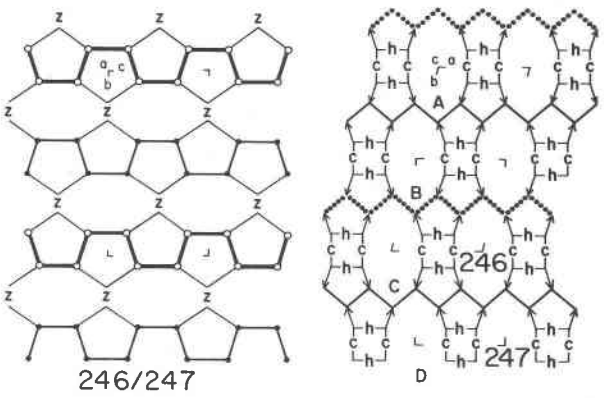

Fig. 5. Two projections of nets 246 and 247. See text for explanation.

Addition of zigzag chains and other structural features

Centered net

Nets 246–257 are selected from the infinity of nets produced by addition of zigzag chains and other structural features to the centered 2D net of pentagons and octagons.

Nets 246 and 247 are the simplest polytypes of an infinite series obtained by placing a zigzag chain at each bridge between adjacent octagons and by converting edges of the pentagons into a horizontal double-crankshaft chain (Fig. 5, left: heavy lines joining circled nodes). The c-axis projection (Fig. 5, right) shows how the 3D net can be represented by conversion of some branches from a 2D net $(4.5.8)_2(5.5.8)_1(5.8.8)_1$ into crankshaft (c) and saw (arrow) chains. Some horizontal branches are retained either as single ones (h) or as components of zigzag chains (heavy lines and dots). There are two choices for attachment of the double-crankshaft chains to the zigzag chains, as is most easily seen by looking at the elongated octagons at the right. Continuation of the oblique sequence ABC gives the monoclinic net 246, while continuation of the zigzag sequence BCD gives orthorhombic net 247. The 3D channel systems are limited by elliptical 8-rings in all directions.

The combination of zigzag chains between the pentagons and stepping-stone 4-rings (s4s) between the octagons produces a multiply-infinite series of 3D nets, two of which are represented by dachiardite (Gottardi and Meier, 1963) and epistilbite (Perrotta, 1967). Although the schematic projections of Figure 6 are convenient for enumeration, the stereoplots of dachiardite and epistilbite (Meier and Olson, 1978) are helpful. The four simplest nets (Merlino, 1978) are projected in Figure 6. There are two choices of height for each s4s in the centered 2D net at the left. The first infinite series, which contains dachiardite (net 248), is based on the same height for d, d′, d″, etc., and similarly for e, e′, e″, for f, f′, f″, and for g, g′, g″; however d, e, f and g may have different heights. The two simplest choices of relative height are shown in the c-axis projection (next diagram). This reveals the same 2D net as in Figure 5, but with a different choice of crankshaft and saw chains. The oblique choice of 4-rings d, e, f yields the monoclinic cell of net 248, and positions p and q would extend that net. The zigzag choice e, f, g yields the orthorhombic cell of net 249 which would extend to positions r and s. Algebraically, this polytypic series can be expressed by giving fractional coordinates along the a-axis (bottom) and the c-axis (left-hand side).

The second infinite series, which contains epistilbite (net 250), has d and d″, *etc.* at the same height along the a-axis (*e.g.*, 1/2) and alternate positions (*e.g.*, d′) displaced by one-half. In the c-axis projection, the 4-rings of horizontal linkages are now represented by continuous and dashed lines (Fig. 5, two right-hand diagrams). Whereas all the s4s labeled d, d′, d″ project onto d for the dachiardite net (248), they project alternately onto two positions for the epistilbite net (250). Again there is an infinite set of choices for s4s of types d, e, f, g, *etc.*, and

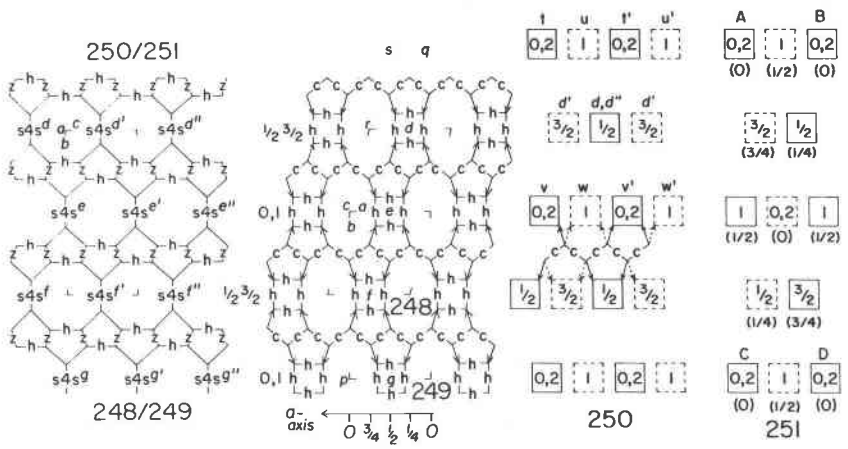

Fig. 6. Projections for nets 248–251. See text for explanation.

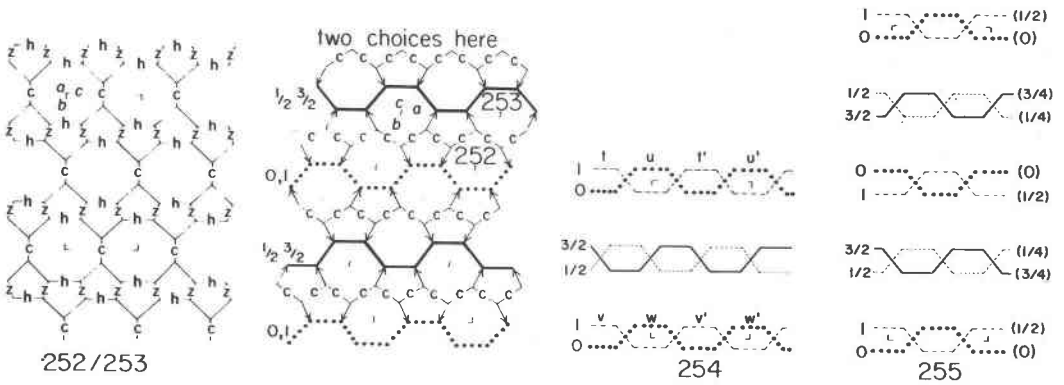

Fig. 7. Projections for nets 252–255. See text for explanation.

the two simplest ones are nets 250 and 251. The unbracketed heights in the two right-hand diagrams refer to the **a**-axis of the extreme left-hand drawing. Net 251 has an orthorhombic cell outlined by ABCD, and doubling of the *a*-repeat results in the bracketed fractions. The zigzag sequence 0, 1/4, 1/2, 3/4 produces the diamond glide planes in the space group *Fddd* (Table 1). Dachiardite (250) has a monoclinic cell with corners at height 0 (t, t′, v, v′) and 1 (u, u′, w, w′).

All nets of these two polytypic series contain crinkled sheets of 6-rings composed of linked crankshaft chains (horizontal rows of c, Fig. 6), as described by Meier (1978) and Merlino (1975). Stacking faults in dachiardite and epistilbite are described by Gellens *et al.* (1982) and Slaughter and Kane (1969). Various related structures described by Kerr (1963), Merlino (1975) and Sherman and Bennett (1973) will be described in a later paper which includes the mordenite net.

Nets 252–255 are the simplest representatives of the infinite polytypic series formed by insertion of zigzag chains between adjacent pentagons and crankshaft chains between adjacent octagons (Fig. 7, left). The **c**-axis projection shows how the zigzag chains along the **a**-axis are replaced by crankshaft chains along the **c**-axis. These c chains are connected by saw chains (arrows) to the horizontal crankshaft chains at two levels (heavy line *vs.* dots). Just as for the dachiardite and epistilbite series, there are two choices. Superposition of the horizontal crankshafts at *c* equals 1/2 and 3/2 or at 0 and 1 gives the polytypic series represented by nets 252 and 253 which are analogous to the 248/249 nets. Displacement of the horizontal crankshafts by *a*/2 (Fig. 7, right-hand diagrams) gives the polytypic series represented by nets 254 and 255 which are analogous to the 250/251 nets. Bracketed fractions are obtained as in Figure 6. Net 254 is monoclinic with cell corners at height O (u, u′, w, w′) and 1 (r, r′, v, v′). The **c**-axis projections of nets 252/253 are based on $(5^27).(57^2)_3$ 2D nets, of which the rectangular one for 3D net 252 is found in the B net of $YCrB_4$ (O'Keefe and Hyde, 1980, Fig. 30a). Crinkled sheets of 6-rings are represented by linked crankshaft chains (horizontal rows of c, Fig. 7).

Finally, for the centered 2D net of pentagons and octagons, Fig. 8 shows projections for the polytypic series represented by nets 256 and 257. Each branch between two pentagons is replaced by a crankshaft in the left-hand drawing, and each branch between two octagons by a zigzag chain. Adjacent crankshafts lie at the same height along the *a*-axis, and become joined by s4s. Staggering the crankshafts by a **a**/2 produces highly-strained nets which are not given here. The *c*-axis projection reveals the same 2D nets found for nets 252 and 253, but with a different set of 3D linkages.

Zigzag net

The zigzag feature produces an asymmetry in the 8-ring (Fig. 1) which leads to nets of greater complexity than those developed from the centered 2D net. All the nets in Figure 9 belong to polytypic series analogous to those of nets 246–257. The zigzag feature precludes simple projection down the **c**-axis. Because the nets are complex and inelegant, they are not given numbers and are not listed in Table 1.

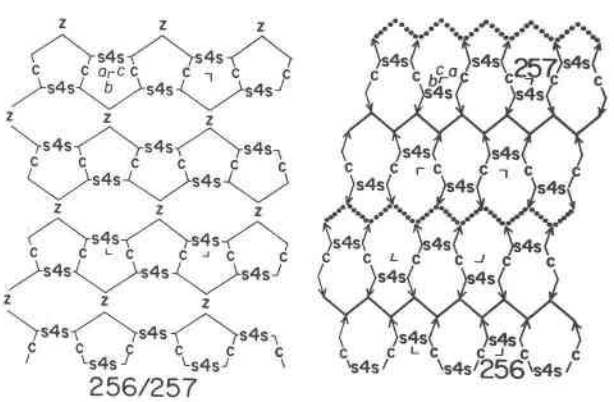

Fig. 8. Projections for nets 256 and 257. See text for explanation. Compare with Fig. 7.

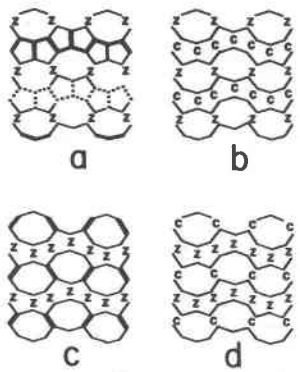

Fig. 9. Projections of nets obtained by addition of zigzag and other linkages to the zigzag 2D net. Heavy lines in a and b show projections of vertical 4-rings. Rows of dots in a show vertical 4-rings displaced with respect to ones shown in heavy line.

Addition of saw chains

All 3D nets obtained by replacing branches of both the centered and zigzag 2D nets of linked pentagons and octagons are complex with some severely distorted polygons. All models were highly strained, and would not adopt a symmetrical shape even after several unit cells had been built. A systematic enumeration was not completed because it became obvious that the models were inelegant and complex. This was disappointing because the models contain channels bounded by 12-rings.

Conclusion

The present enumeration of 4-connected 3D nets based on 2D nets containing pentagons and octagons has revealed many infinite series of nets which are not only polytypic within a series but also between some series. Forty of the simpler nets were selected for detailed description, and four are represented by bikitaite, dachiardite, epistilbite and the $CsAlSi_5O_{12}$ structure. Because the nets can be distorted considerably, it would be wise to allow a tolerance of at least 5% in cell edges and 5° in cell angle when attempting to obtain a match with cell dimensions of an unknown structure. Although the four observed structures are structurally elegant, they are not really simple; thus there are three types of circuit symbols for epistilbite and dachiardite. Furthermore, some of the simpler theoretical nets do not have observed counterparts. It is obvious that crystal-chemical factors are important in selection of the theoretical nets for actual crystal structures, and that there is no simple route to prediction of tetrahedral frameworks.

Acknowledgments

We thank Nancy Weber for typing, and Union Carbide Corporation and the National Science Foundation (grant CHE 80-23444) for support.

References

Araki, T. (1980) Crystal structure of a cesium aluminosilicate, $Cs[AlSi_5O_{12}]$. Zeitschrift für Kristallographie, 152, 207–213.

Gellens, L. R., Price, G. D. and Smith, J. V. (1982) The structural relation between svetlozarite and dachiardite. Mineralogical Magazine, 45, 157–161.

Gottardi, G. and Meier, W. M. (1963) The crystal structure of dachiardite. Zeitschrift für Kristallographie, 119, 53–64.

Kerr, I. S. (1963) Possible structures related to mordenite. Nature, 197, 1194–1195.

Kocman, V., Gait, R. I. and Rucklidge J. (1974) The crystal structure of bikitaite, $Li(AlSi_2O_6) \cdot H_2O$. American Mineralogist, 59, 71–78.

Meier, W. M. (1978) Constituent sheets in the zeolite frameworks of the mordenite group. In L. B. Sand and F. Mumpton, Eds., Natural Zeolites, p. 99–103. Pergamon, New York.

Meier, W. M. and Olson, D. H. (1978) Atlas of zeolite structure types. Polycrystal Book Service, Pittsburgh, PA.

Merlino, S. (1975) Le strutture dei *tettosilicati*. Rendiconti Societa Italiana di Mineralogia e Petrologia, 31, 513–540.

O'Keefe, M. and Hyde, B. G. (1980) Plane nets in crystal chemistry. Philosophical Transactions of the Royal Society of London, 295, 553–618.

Perrotta, A. J. (1967) The crystal structure of epistilbite. Mineralogical Magazine, 36, 480–490.

Sherman, J. D. and Bennett, J. M. (1973) Framework structures related to the zeolite mordenite. Advances in Chemistry Series, 121, 52–65. American Chemical Society, Washington, D. C.

Slaughter, M. and Kane, W. T. (1969) The crystal structure of disordered epistilbite. Zeitschrift für Kristallographie, 130, 68–87.

Smith, J. V. (1977) Enumeration of 4-connected 3-dimensional nets and classification of framework silicates. I. Perpendicular linkage from simple hexagonal net. American Mineralogist, 62, 703–709.

Smith, J. V. (1978) Enumeration of 4-connected 3-dimensional nets and classification of framework silicates, II. Perpendicular and near-perpendicular linkages from 4.8^2, 3.12^2 and 4.6.12 nets. American Mineralogist, 63, 960–969.

Smith, J. V. (1979) Enumeration of 4-connected 3-dimensional nets and classification of framework silicates, III. Combination of helix, and zigzag, crankshaft and saw chains with simple 2D nets. American Mineralogist, 64, 551–562.

Smith, J. V. and Bennett, J. M. (1981) Enumeration of 4-connected 3-dimensional nets and classification of framework silicates: the infinite set of ABC-6 nets; the Archimedean and σ-related nets. American Mineralogist 66, 777–788.

Manuscript received, December 29, 1982;
accepted for publication, July 29, 1983.